

Charged Particle Motion Around Rotating Black Hole in Braneworld Immersed in Magnetic Field

Ahmadjon Abdujabbarov* and Bobomurat Ahmedov†

Institute of Nuclear Physics, Ulughbek, Tashkent 100214, Uzbekistan

Ulugh Beg Astronomical Institute, Astronomicheskaya 33, Tashkent 100052, Uzbekistan

Inter University Centre for Astronomy & Astrophysics, Post Bag 4, Pune 411007, India

(Dated: August 19, 2018)

Analytical solutions of Maxwell equations in background spacetime of black hole in braneworld immersed in external uniform magnetic field have been found. Influence of both magnetic and brane parameters on effective potential of the radial motion of charged test particle around slowly rotating black hole in braneworld immersed in uniform magnetic field has been investigated by using Hamilton-Jacobi method. Exact analytical solution for dependence of the radius of the innermost stable circular orbits (ISCO) r_{ISCO} from brane parameter for motion of test particle around nonrotating isolated black hole in braneworld has been derived. It has been shown that radius r_{ISCO} is monotonically growing with the increase of module of brane tidal charge. Comparison of the predictions on r_{ISCO} of the brane world model and of the observational results of ISCO from relativistic accretion disks around black holes provided upper limit for brane tidal charge $\lesssim 10^9 \text{cm}^2$.

PACS numbers: 04.50.-h, 04.40.Dg, 97.60.Gb

I. INTRODUCTION

The idea that our Universe might be a three-brane [1], embedded in a higher dimensional spacetime, has recently attracted much attention. For astrophysical interests, static and spherically symmetric exterior vacuum solutions of the brane world models were initially proposed by Dadhich et al [2, 3] which have the mathematical form of the Reissner-Nordström solution, in which a tidal Weyl parameter Q^* plays the role of the electric charge squared of the general relativistic solution. The so-called DMPR solution was obtained by imposing the null energy condition on the three-brane for a bulk having nonzero Weyl curvature.

Observational possibilities of testing the brane world black hole models at an astrophysical scale have intensively discussed in the literature during the last years, for example through the gravitational lensing [4, 5, 6, 7, 8, 9], the motion of test particles [10] and the classical tests of general relativity (perihelion precession, deflection of light and the radar echo delay) in the Solar system [11]. The role of the tidal charge in orbital models of high-frequency quasiperiodic oscillations observed in neutron star binary systems has been also studied [12]. In the paper [13] the energy flux, the emission spectrum and accretion efficiency from the accretion disks around several classes of static and rotating brane-world black holes have been obtained. The complete set of analytical solutions of the geodesic equation of massive test particles in higher dimensional spacetimes which can be applied to braneworld models is provided in the recent paper [14]. Recently the deflection angle of light rays caused by a massive black hole in braneworld in the weak lensing approach has been derived, up to the second order in perturbation theory [15, 16].

A braneworld corrections to the charged rotating black holes and to the perturbations in the electromagnetic potential around black holes are studied in [17, 18]. Our preceding paper [19] was devoted to the stellar magnetic field configurations of relativistic stars in dependence on brane tension. Here we plan to study electromagnetic fields and particle motion around rotating black hole in braneworld immersed in uniform magnetic field. The study of the particle orbits could provide an opportunity for constraining the allowed parameter space of solutions, and to provide a deeper insight into the physical nature and properties of the corresponding spacetime metrics. Therefore, this may open up the possibility of testing brane world models by using astronomical and astrophysical observations around black holes, in particular observationally measured ISCO radii around black holes in principle may give definite constraints on the numerical value of the brane tidal charge.

The paper is organized as follows. In section II we look for exact solutions of vacuum Maxwell equations in spacetime of the rotating black hole in braneworld immersed in uniform magnetic field. In the next section III motion of charged particles around black hole in braneworld immersed in uniform magnetic field has been studied in slow

*Electronic address: abahmadjon@yahoo.com

†Electronic address: ahmedov@astrin.uzsci.net

rotation approximation. We obtain the effective potential for any particle with a specific angular momentum, orbiting around the black hole, as a function of the magnetic field, and of the tidal charge of the black hole. Exact expression for dependence of radius of innermost stable circular orbit from brane charge has been found in section IV for the test particle moving in the equatorial plane of the black hole in braneworld when both rotation and magnetic parameters are neglected for the simplicity of calculations. Then we present clear derivation of the capture cross section of slowly moving test particles by black hole in braneworld. The exact expressions for critical angular momentum of the test particle and corresponding radius of particle unstable circular orbits around the black hole have been presented. For different tidal charges, the values of the radii of the marginally stable orbits around black hole in braneworld, are also plotted. The conclusion and discussion of the obtained results can be found in section V.

We use in this paper a system of units in which $c = 1$, a space-like signature $(-, +, +, +)$ and a spherical coordinate system (t, r, θ, φ) . Greek indices are taken to run from 0 to 3, Latin indices from 1 to 3 and we adopt the standard convention for the summation over repeated indices. We will indicate vectors with bold symbols (*e.g.* \mathbf{B}).

II. ROTATING BLACK HOLE IN BRANEWORLD IMMERSSED IN UNIFORM MAGNETIC FIELD

Spacetime metric of the rotating black hole in braneworld in coordinates t, r, θ, φ takes form (see *e.g.*, [17])

$$ds^2 = -\frac{\Delta - a^2 \sin^2 \theta}{\Sigma} dt^2 + \frac{(\Sigma + a^2 \sin^2 \theta)^2 - \Delta a^2}{\Sigma} \sin^2 \theta d\varphi^2 + \frac{\Sigma}{\Delta} dr^2 + \Sigma d\theta^2 - 2\frac{\Sigma + a^2 \sin^2 \theta - \Delta}{\Sigma} a \sin^2 \theta d\varphi dt, \quad (1)$$

where $\Sigma = r^2 + a^2 \cos^2 \theta$, $\Delta = r^2 + a^2 - 2Mr + Q^*$, Q^* is the bulk tidal charge, M is the total mass and a is related to the angular momentum of the black hole.

It is not difficult to show that the electromagnetic corrections created by the external magnetic field being proportional to the electromagnetic energy density are rather small in most black holes. Indeed if B is the external magnetic field around black hole in braneworld of total mass M at radius r , these corrections are at most

$$\frac{B^2 r^3}{8\pi M c^2} \simeq 7 \cdot 10^{-4} \left(\frac{B}{10^{12} \text{ G}} \right)^2 \left(\frac{10^6 M_\odot}{M} \right) \left(\frac{r}{1.5 \cdot 10^6 \text{ km}} \right)^3. \quad (2)$$

Here we exploit the existence in this spacetime of a timelike Killing vector $\xi_{(t)}^\alpha$ and spacelike one $\xi_{(\varphi)}^\alpha$ being responsible for stationarity and axial symmetry of geometry, such that they satisfy the Killing equations $\xi_{\alpha;\beta} + \xi_{\beta;\alpha} = 0$, and consequently the wave-like equations (in vacuum spacetime) $\square \xi^\alpha = 0$, which gives a right to write the solution of vacuum Maxwell equations $\square A^\mu = 0$ for the vector potential A_μ of the electromagnetic field in the Lorentz gauge in the simple form $A^\alpha = C_1 \xi_{(t)}^\alpha + C_2 \xi_{(\varphi)}^\alpha$. [20] The constant $C_2 = B/2$, where gravitational source is immersed in the uniform magnetic field \mathbf{B} being parallel to its axis of rotation. The value of the remaining constant $C_1 = aB$ can be easily calculated from the asymptotic properties of spacetime (1) at the infinity (see *e.g.* our preceding paper [21] for the details of typical calculations).

Finally the components of the 4-vector potential A_α of the electromagnetic field will take a form

$$A_0 = \frac{aB}{2\Sigma} [(2 - \sin^2 \theta)(a^2 \sin^2 \theta - \Delta) - \Sigma \sin^2 \theta], \quad A_1 = A_2 = 0, \\ A_3 = \frac{B \sin^2 \theta}{2\Sigma} [(\Delta - \Sigma - a^2)(2 - \sin^2 \theta)a^2 + \Sigma(\Sigma + \sin^2 \theta)]. \quad (3)$$

The nonvanishing orthonormal components of the electromagnetic fields measured by zero angular momentum observers (ZAMO) with the four-velocity components

$$(u^\alpha)_{\text{ZAMO}} \equiv \frac{K}{\sqrt{\Delta\Sigma}} \left(1, 0, 0, \frac{\Sigma a^2 \sin^2 \theta}{\Delta - a^2 \sin^2 \theta} - 1 \right), \quad (u_\alpha)_{\text{ZAMO}} \equiv \frac{\sqrt{\Delta\Sigma}}{K} (1, 0, 0, 0) \quad (4)$$

are given by expressions

$$E^{\hat{r}} = \frac{aB}{\Sigma^2} \left\{ 2(M-r) + M \sin^2 \theta + \frac{\sin^4 \theta}{\Delta - a^2 \sin^2 \theta} (\Sigma - \Delta + a^2 \sin^2 \theta) \left[r\Sigma + a^2(2 - \sin^2 \theta) \right. \right. \\ \left. \left. \times \frac{r\Delta - a^2 r + (M-r)\Sigma}{\Sigma} \right] + \frac{r}{\Sigma} (2 - \sin^2 \theta) [\Sigma^2 + (\Delta - a^2 \sin^2 \theta)(2 - \sin^2 \theta)] \right\} K, \quad (5)$$

$$E^{\hat{\theta}} = \frac{aB \sin 2\theta}{2\Sigma^2 \sqrt{\Delta}} \left\{ a^2 \sin^2 \theta - \Delta - \Sigma + \frac{a^2 \sin^2 \theta - \Delta + \Sigma}{\Sigma} a^2 (2 - \sin^2 \theta) + \frac{a^2 \sin^2 \theta - \Delta + \Sigma}{\Delta \csc^2 \theta - a^2} [(\Sigma + a^2 \right. \\ \left. \times (2 + \cos^2 \theta) - \Delta) a^2 \sin^2 \theta + \Sigma(\Sigma + a^2 \sin^2 \theta) - \frac{\Sigma - \Delta + a^2}{\Sigma} a^2 (\Sigma + a^2 \sin^2 \theta)(2 - \sin^2 \theta)] \right\} K, \quad (6)$$

$$B^{\hat{r}} = \frac{B \csc \theta}{2K\Sigma} \left[(\Sigma + a^2(2 + \cos^2 \theta) - \Delta) a^2 \sin^2 \theta + \Sigma(\Sigma + a^2 \sin^2 \theta) \right. \\ \left. - \frac{\Sigma - \Delta + a^2}{\Sigma} a^2 (\Sigma + a^2 \sin^2 \theta)(2 - \sin^2 \theta) \right], \quad (7)$$

$$B^{\hat{\theta}} = \frac{B \sin \theta \sqrt{\Delta}}{K\Sigma} \left[r\Sigma + a^2(2 - \sin^2 \theta) \frac{r\Delta - a^2 r + (M-r)\Sigma}{\Sigma} \right], \quad (8)$$

which depend on angular momentum and tidal charge in complex way and where we have used $K = ((\Sigma + a^2 \sin^2 \theta)^2 - a^2 \Delta \sin^2 \theta)^{1/2}$. In the limit of flat spacetime, i.e. for $M/r \rightarrow 0$, $Ma/r^2 \rightarrow 0$ and $Q^*/r^2 \rightarrow 0$, expressions (5)–(8) give the following limiting expressions: $B^{\hat{r}} = B \cos \theta$, $B^{\hat{\theta}} = B \sin \theta$, $E^{\hat{r}} = E^{\hat{\theta}} = 0$, which coincide with the solutions for the homogeneous magnetic field in Newtonian spacetime. Here $\hat{}$ stands for orthonormal components of the electric and magnetic fields. Uniform magnetic field in the background of a five dimensional black hole has been extensively studied in [22]. In particular authors presented exact expressions for two forms of electromagnetic tensor and the electrostatic potential difference between the event horizon of five dimensional black hole and the infinity.

III. CHARGED PARTICLE MOTION IN THE VICINITY OF ROTATING BLACK HOLE IN BRANEWORLD

In this section we investigate in detail the motion of charged particles around a rotating black hole in braneworld in an external magnetic field given by 4-vector potential (3) with the aim to find a way for astrophysical evidence for either the existence or nonexistence of tidal charge Q^* . For simplicity of calculations we assume parameter a to be small, and obtain the exterior metric for slowly rotating compact object in the braneworld in the following form

$$ds^2 = -A^2 dt^2 + H^2 dr^2 + r^2 d\theta^2 + r^2 \sin^2 \theta d\varphi^2 - 2\tilde{\omega}(r) r^2 \sin^2 \theta dt d\varphi, \quad (9)$$

here

$$A^2(r) \equiv \left(1 - \frac{2M}{r} + \frac{Q^*}{r^2} \right) = H^{-2}(r), \quad r > R, \quad (10)$$

is the Reissner-Nordström-type exact solution [2] for the metric outside the gravitating object and $\tilde{\omega}(r) = \omega(1 - Q^*/2rM) = 2Ma/r^3(1 - Q^*/2rM)$.

The Hamilton-Jacobi equation

$$g^{\mu\nu} \left(\frac{\partial S}{\partial x^\mu} + eA_\mu \right) \left(\frac{\partial S}{\partial x^\nu} + eA_\nu \right) = -m^2, \quad (11)$$

for motion of the charged test particles with mass m and charge e is applicable as a useful computational tool only when separation of variables can be effected.

Since spacetime of the rotating object in braneworld admits such separation of variables (see e.g. [23]) we shall study the motion around source described with metric (9) using the Hamilton-Jacobi equation when the action S can be decomposed in the form

$$S = -\mathcal{E}t + \mathcal{L}\varphi + S_{r\theta}(r, \theta), \quad (12)$$

since the energy \mathcal{E} and the angular momentum \mathcal{L} of a test particle are constants of motion in the spacetime (9).

Therefore the Hamilton-Jacobi equation (11) with action (12) implies the equation for inseparable part of the action as

$$\begin{aligned} & \frac{1}{2A^2} \left[\mathcal{E} + \frac{a}{r} \left(\frac{2M\mathcal{L}}{r^2} - \frac{Q^*\mathcal{L}}{r^3} + A^2 eB \right) \right] \left[2\mathcal{E} + aeBA^2 - aeB \left(\frac{2M}{r} - \frac{Q^*}{r^2} \right) \sin^2 \theta \right] + \left(\mathcal{L} + \frac{1}{2} eBr^2 \sin^2 \theta \right) \\ & \times \left[\frac{eB}{2} + \frac{\mathcal{L}}{r^2 \sin^2 \theta} - \frac{a\mathcal{E}}{r^2 A^2} \left(\frac{2M}{r} - \frac{Q^*}{r^2} \right) \right] + A^2 \left(\frac{\partial S_{r\theta}}{\partial r} \right)^2 + \frac{1}{r^2} \left(\frac{\partial S_{r\theta}}{\partial \theta} \right)^2 = -m^2. \end{aligned} \quad (13)$$

It is not possible to separate variables in this equation in general case but it can be done for the motion in the equatorial plane $\theta = \pi/2$ when the equation for radial motion takes form

$$\left(\frac{dr}{d\sigma} \right)^2 = \mathcal{E}^2 - 1 - 2V_{\text{eff}}(\mathcal{E}, \mathcal{L}, r, \epsilon, a, Q^*). \quad (14)$$

Here σ is the proper time along the trajectory of a particle, \mathcal{E} and \mathcal{L} are energy and angular momentum per unit mass m and

$$V_{\text{eff}}(\mathcal{E}, \mathcal{L}, r, \epsilon, a, Q^*) = \frac{a\mathcal{E}\mathcal{L}}{r^2} \left(\frac{2M}{r} - \frac{Q^*}{r^2} \right) + \left(\frac{\mathcal{L}^2}{2r^2} + \frac{\epsilon\mathcal{L}}{2} + \frac{\epsilon^2 r^2}{8} + a\mathcal{E}\epsilon \right) \left(1 - \frac{2M}{r} + \frac{Q^*}{r^2} \right) - \frac{M}{r} + \frac{Q^*}{2r^2} \quad (15)$$

is effective potential, where $\epsilon = eB/m$ is the magnetic parameter.

Fig. 1 shows the radial dependence of effective potential of the radial motion of charged particle on equatorial plane of slowly rotating black hole in braneworld immersed in uniform magnetic field for different values of parameter of magnetic field (left graph) and tidal charge (right one). One can obtain now how magnetic and brane parameters change the character of the motion of the charged particle. Both magnetic and tidal parameters cause to shift the shape of the effective potential to the observer in infinity that means the minimum distance of the charged particles to the central object increases. As module of the tidal charge increases parabolic and hyperbolic orbits start to become unstable circular orbits, while magnetic parameter gives opposite effect (Fig. 1) (see e.g. our preceding research [21]). Thus the radial profile of V_{eff} for different values of the tidal charge Q^* , running between -0.01 and -0.03 shows that by increasing module of Q^* from 0.01 to 0.03 we also lower the potential barrier, as compared to the Schwarzschild case, as expected for the potential of the Reissner-Nordström type black holes.

The choice of the brane parameter's sign is stipulated according to the following reason: the negative bulk cosmological constant contributes to acceleration towards the brane, reflecting its confining role on the gravitational field. In order for U to reinforce confinement, it must be negative. An effective energy density $U = \kappa Q^*/r^4$ on the brane arising from the free gravitational field in the bulk, where κ is the positive constant, needs not be positive. Indeed, $U < 0$ is the natural case. In other words, negative tidal charge $Q^* < 0$ is the physically more natural case. Furthermore, $Q^* < 0$ ensures that the singularity is spacelike, as in the Schwarzschild solution, whereas $Q^* > 0$ leads to a timelike singularity, which amounts to a qualitative change in the nature of the general relativistic Schwarzschild solution (see for more details [2]).

IV. MOTION OF TEST PARTICLE AROUND BLACK HOLE IN BRANEWORLD

In order to find exact analytical solution for radius r_{ISCO} we assume that external magnetic field is absent and black hole in braneworld is nonrotating when metric (9) can be written in the diagonal form as

$$ds^2 = -\frac{\Delta}{r^2} dt^2 + \frac{r^2}{\Delta} dr^2 + r^2 d\theta^2 + r^2 \sin^2 \theta d\varphi^2, \quad (16)$$

where $\Delta = r^2 - 2Mr + Q^*$ does not include terms being proportional to angular momentum of black hole. Now using the Hamilton-Jacobi method described in previous section III one can easily find equation of motion of test particle in the equatorial plane of the black hole in braneworld as

$$\frac{dt}{d\sigma} = \mathcal{E} \frac{r^2}{\Delta}, \quad (17)$$

$$\left(\frac{dr}{d\sigma} \right)^2 = \mathcal{E}^2 - \frac{\Delta}{r^2} \left(1 + \frac{\mathcal{L}^2}{r^2} \right), \quad (18)$$

$$\frac{d\varphi}{d\sigma} = \frac{\mathcal{L}}{r^2}. \quad (19)$$

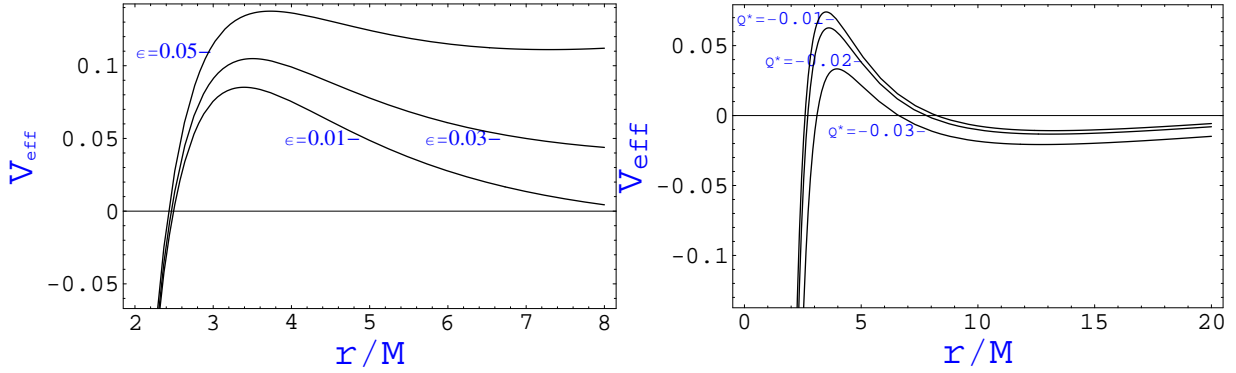


FIG. 1: Radial dependence of the effective potential of the radial motion of the charged particles around slowly rotating black hole in braneworld immersed in uniform magnetic field for the different parameter of the magnetic field ϵ (left graph) and tidal charge Q^* (right graph) .

Using the equations (18) and (19) and introducing new variable $u = 1/r$ one can obtain the following equation

$$\left(\frac{du}{d\varphi}\right)^2 = -Q^*u^4 + 2Mu^3 - \left(1 + \frac{Q^*}{\mathcal{L}^2}\right)u^2 + \frac{2M}{\mathcal{L}^2}u - \frac{1 - \mathcal{E}^2}{\mathcal{L}^2} = f(u), \quad (20)$$

which defines the trajectory of the test particle around black hole in braneworld. The condition of occurrence of circular orbits is:

$$f(u) = 0, \quad f'(u) = 0.$$

From these equations, it follows that energy \mathcal{E} and angular momentum \mathcal{L} of a circular orbit of radius $r_c = u_c$ is given by

$$\mathcal{E}^2 = \frac{(1 - 2Mu + Q^*u^2)^2}{1 - 3Mu + 2Q^*u^2}, \quad (21)$$

$$\mathcal{L}^2 = \frac{M - Q^*u}{2Q^*u^3 - 3Mu^2 + u}. \quad (22)$$

Fig. 2 shows the radial dependence of both the energy and the angular momenta of the test particle moving on circular orbits in the equatorial plane. One can easily see that presence of the brane parameter forces test particle to have bigger energy and angular momentum in order to be kept on its circular orbit. It is a consequence of the increase of the gravitational potential of the central object in braneworld.

From equations (21) and (22) one can easily find minimum radius for circular orbits r_{mc}

$$r_{mc} > \frac{4Q^*}{3M - \sqrt{9M^2 - 8Q^*}}, \quad (23)$$

or if we expand this expression in degrees of Q^*/M^2 , it takes the following form:

$$r_{mc} \approx 3M - \frac{2Q^*}{3M} - \frac{4Q^{*2}}{27M^3} + \mathcal{O}\left(\frac{Q^{*3}}{M^5}\right). \quad (24)$$

In the limiting case when Q^* tends to zero $r_{mc} = 3M$ which coincides with the Schwarzschild limit. The minimum radius for a stable circular orbit will occur at point of inflexion of the function $f(u)$, or in other words we must supplement conditions $f(u) = f'(u) = 0$ with the equation $f''(u) = 0$. Then one can easily obtain the equation

$$4Q^{*2}u^3 - 9MQ^*u^2 + 6M^2u - M = 0, \quad (25)$$

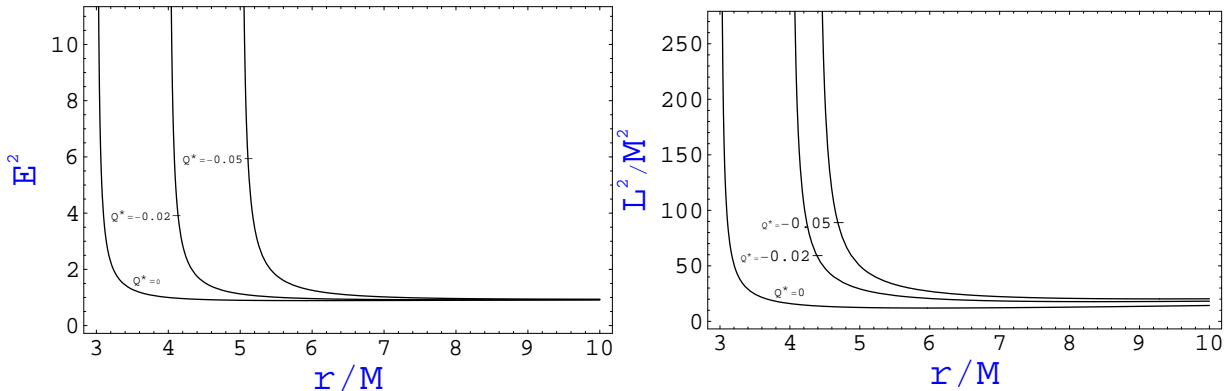


FIG. 2: Radial dependence of energy (left graph) and angular momentum (right graph) of circular orbits around black hole in braneworld for the different values of the brane tension Q^* . For comparison we have also plotted the Schwarzschild dependence, corresponding to $Q^* = 0$.

and its solution in the form

$$r = \frac{4Q^*}{3M + \sqrt[3]{A-B} + \sqrt[3]{A+B}} \equiv r_{\text{ISCO}} , \quad (26)$$

where

$$A = 8MQ^* - 9M^3, \quad B = 4\sqrt{(4MQ^* - 5M^3)(MQ^* - M^3)} , \quad (27)$$

or if we expand this expression in degrees of Q^*/M^2 , it takes the following form:

$$r_{\text{ISCO}} \approx 6M - 1.5\frac{Q^*}{M} + 0.0078\frac{Q^{*2}}{M^3} + \mathcal{O}\left(\frac{Q^{*3}}{M^5}\right) . \quad (28)$$

To the best of our knowledge the analytical expression (26) is original one. It defines the limit of the stability of innermost circular orbit in vicinity of black hole in braneworld. Numerical solutions with similar results for r_{ISCO} around rotating black hole in braneworld and circular orbits in accretion disks have been studied in papers [17] and [13], respectively.

The dependence of the minimum radius for circular orbits r_{mc} and radius of ISCO around black hole from the brane tidal charge is plotted in the Fig. 3, where the values related to the Schwarzschild black hole correspond to $Q^* = 0$. One can easily see from the plots that presence of the tidal charge forces the radius of the stable orbits to be shifted away from the central object in the direction of an observer at infinity which confirms the earlier results of Aliev & Gümrükçüoğlu [17].

The variation of Q^* also modifies the position of the marginally stable orbit, as shown by the shift of the ISCO, which is presented in the left plot in the Fig. 3. The negative decreasing charges lead to the increase of ISCO radius. By decreasing the value of Q^* from 0 to -5, we shift the radius of ISCO to bigger and bigger values. The lower values of the potential for Q^* involve a lower specific energy of the orbiting particles. As we decrease Q^* from 0 to -5, ISCO radius is increasing from values greater than the radius of the marginally stable orbit for the Schwarzschild geometry to bigger ones. The efficiency has an opposite trend with compare to angular momentum: for negative tidal charges it has bigger values than in the case of the Schwarzschild black holes.

Next, we will give clear derivation of the capture cross section of slowly moving test particles by black hole in braneworld (Slow motion means that $\mathcal{E} \simeq 1$ at the infinity.). The critical value of the particle's angular momentum, \mathcal{L}_{cr} , hinges upon the existence of a multipole root of the polynomial $f(u)$ in (20) [24]. For convenience hereafter we rewrite the equation (20) in terms of dimensionless parameters as radial coordinate $r \rightarrow r/M$, momentum $\mathcal{L} \rightarrow \mathcal{L}/M$ and tidal charge $Q^* \rightarrow Q^*/M^2$:

$$r^3 - \frac{\mathcal{L}^2 + Q^*}{2}r^2 + \mathcal{L}^2r - \frac{Q^*\mathcal{L}^2}{2} = 0 . \quad (29)$$

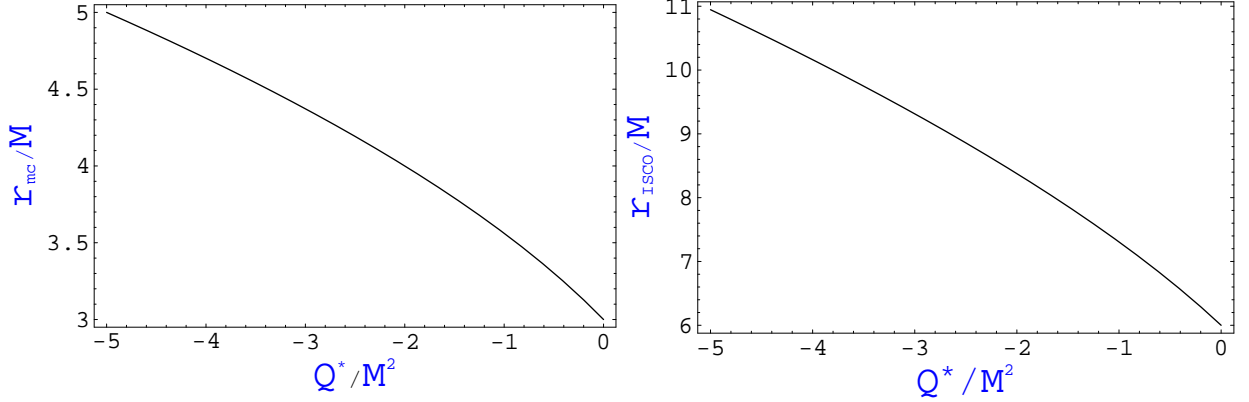


FIG. 3: Dependence of the lower limit for radiuses of circular orbits r_{mc} (left graph) and ISCO r_{ISCO} (right graph) from the tidal charge Q^* .

Cubic equation (29) has a multiple root if and only if its discriminant vanishes. After simple algebraic transformations one can easily obtain the following equation for particle angular momentum

$$\mathcal{L}^6(1 - Q^*) - \mathcal{L}^4(3Q^{*2} - 20Q^* + 16) - \mathcal{L}^2Q^{*2}(8 + 3Q^*) - Q^{*4} = 0, \quad (30)$$

which has an exact solution in the form

$$\mathcal{L}_{cr}^2 = \begin{cases} \sqrt[3]{-B_1/2 + \sqrt{D}} + \sqrt[3]{-B_1/2 - \sqrt{D}} - \frac{(20Q^* - 3Q^{*2} - 16)^2}{3(1 - Q^*)}, & D \geq 0; \\ 2\sqrt{\frac{-A_1}{3}} \cos\left\{\frac{1}{3} \arccos\left[-B_1/(2\sqrt{-(A_1/3)^2})\right]\right\} - \frac{(20Q^* - 3Q^{*2} - 16)^2}{3(1 - Q^*)}, & D < 0. \end{cases} \quad (31)$$

Here we have introduced the following notations

$$\begin{aligned} A_1 &= -\frac{(20Q^* - 3Q^{*2} - 16)^2}{3(1 - Q^*)^2} - \frac{8Q^{*2} + 3Q^{*3}}{1 - Q^*}, \\ B_1 &= 2\frac{(20Q^* - 3Q^{*2} - 16)^2}{27(1 - Q^*)^3} - \frac{(20Q^* - 3Q^{*2} - 16)^2(8Q^{*2} + 3Q^{*3})}{1 - Q^*} - \frac{Q^{*4}}{1 - Q^*}, \\ D &= \frac{A_1^3}{27} + \frac{B_1^2}{4}. \end{aligned}$$

In the limiting case, i.e. when tidal charge vanishes the solution of the equation (30) is $\mathcal{L} = 4$, which coincides with critical angular momentum for particle capture cross section for Schwarzschild black hole [25]. As a particle having a critical angular momentum travels from infinity towards the black hole in braneworld, it spirals into an unstable circular orbit of radius given as

$$r_{uc} = 2\sqrt[3]{\left(\frac{\mathcal{L}^2 + Q^*}{6}\right)^3 - \mathcal{L}\left(\frac{\mathcal{L}^2 + Q^*}{6}\right) + \mathcal{L}^2Q^* + \frac{\mathcal{L}^2 + Q^*}{6}}. \quad (32)$$

Finally in Fig. 4 we present the shapes of different kinds of trajectories of test particles around black hole in braneworld, which are given by equation (20). The trajectories of test particles falling to the central black hole in braneworld for different values of the brane parameter are shown in Fig. 4 a). From the plot one can obtain that increase of the module of the brane parameter causes orbits shift to an observer at the infinity, which is a consequence of increase of the radius of the event horizon by braneworld effects. Fig. 4 b) illustrates the sample of unstable circular orbits of the particles, while Fig. 4 c) shows the shape of the circular orbits around black hole in the braneworld.

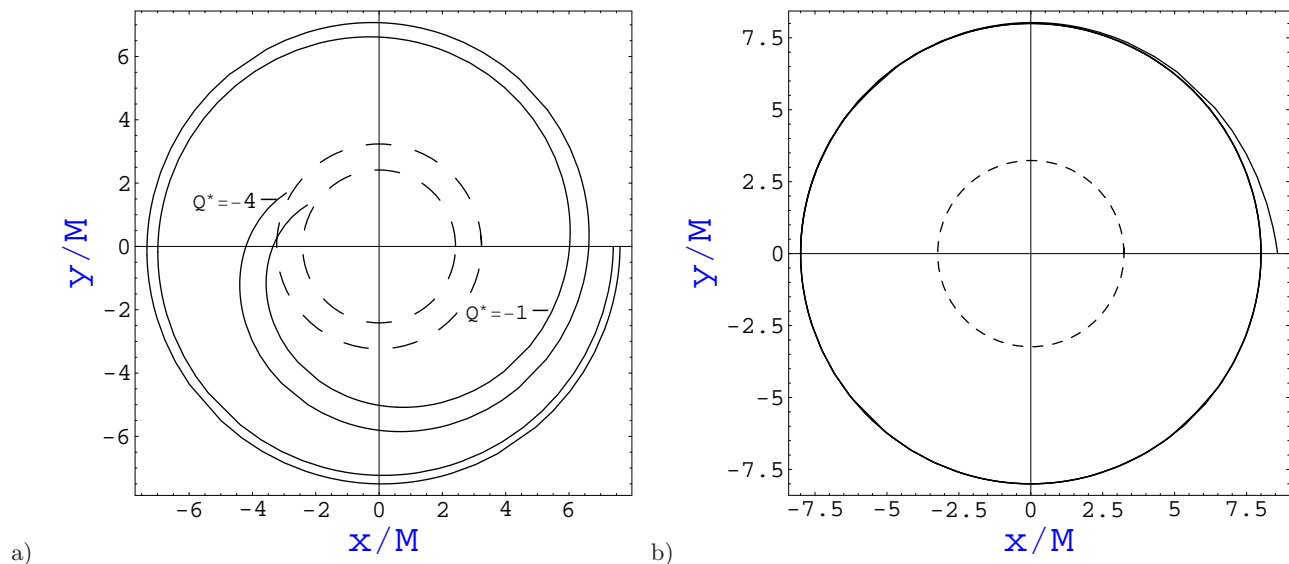


FIG. 4: a). Orbits of the test particle falling into central black hole for different values of the tidal charge Q^* . b). Stable circular orbit of the test particle around black hole in braneworld. In all plots horizons are shown with dash lines.

V. CONCLUSION

We have concentrated here on the basic physical properties of particle motion and magnetic field in the background spacetime metric of the braneworld black holes. Motivation of this research is caused by the fact that testing strong field gravity and the detection of the possible deviations from standard general relativity, signaling the presence of new physics, remains one of the most important objectives of observational astrophysics. Because of their compact nature, black holes provide an ideal environment to perform precise relativistic measurements, in particular the observational possibilities for testing the DMPR solution of the vacuum field equations in brane world models.

Here the physical parameters of the effective potential, and ISCO have been explicitly obtained for several values of the parameters characterizing the vacuum DMPR solution of the field equations in the braneworld models. We have found original exact expression for the lower limit of innermost stable circular orbits of test particle around black hole in braneworld (Before ISCO behavior in braneworld models has been investigated only numerically [13, 17].). Then we have plotted the dependence of the ISCO radius from the brane tidal charge and particle trajectories around black hole in braneworld.

The best constraints on the braneworld black hole parameters were recently obtained from the classical tests of general relativity (perihelion precession, deflection of light, and the radar echo delay, respectively) [11]. The existing observational solar system data on the perihelion shift of Mercury, on the light bending around the Sun (obtained using long-baseline radio interferometry), and ranging to Mars using the Viking lander, were applied to the relativistic in DMPR spacetime, can constrain the numerical values of the brane parameter. The strongest limit $|Q^*| \lesssim 10^8 \text{cm}^2$ was obtained from the Mercury's perihelion precession.

The recent measurements of the ISCO radius in accretion disks around black holes may also give alternate constraints on the numerical values of the brane tidal charge. All the astrophysical quantities related to the observable properties of the accretion disk can be obtained from the black hole metric and observations in the near infrared or X-ray bands have provided important information about the spin of the black holes [26, 27]. It was stated that rotating black holes have spins in the range $0.5 \lesssim a \lesssim 1$ that is according to the observations ISCO radii are essentially shifted towards the central objects and there is no any effect measured from the brane tidal charge which acts in the opposite direction.

Because of the differences in the spacetime structure, the brane world black holes present some important differences with respect to their disc accretion properties, as compared to the standard general relativistic Schwarzschild and Kerr cases. Therefore, the study of the innermost stable orbits in the vicinity of compact objects is a powerful indicator of their physical nature. Since the ISCO radius in the case of the braneworld black holes is different as compared to the standard general relativistic case, the astrophysical determination of these physical quantities could discriminate, at least in principle, between the different gravity theories, and give some constrains on the existence of the extra dimensions. Finally, since there was no braneworld effect on stable orbits around black holes on the scale of a order of 10^8cm^2 , we may conclude that from astrophysical point of view on the base of comparison of observations of ISCO in accretion disks around black holes and ISCO analysis around black hole in braneworld that brane tidal charge has an

upper limit $\lesssim 10^9 \text{cm}^2$. We roughly estimated that one order less magnitude of Q^* may not affect on the observational data on ISCO data around black holes.

Acknowledgments

Authors gratefully thank Naresh Dadhich for his invaluable help, extensive discussions, editing the text and making important corrections and comments. They also thank Valeria Kagramanova for useful discussions. Authors thank the IUCAA for warm hospitality during their stay in Pune and AS-ICTP for the travel support through BIPTUN program. This research is supported in part by the UzFFR (projects 5-08 and 29-08) and projects FA-F2-F079 and FA-F2-F061 of the UzAS. This work is partially supported by the ICTP through the OEA-PRJ-29 project and the Regular Associateship grant.

-
- [1] L. Randall and R. Sundrum, Phys. Rev. Lett. **83**, 3370; 4690 (1999).
 - [2] N. K. Dadhich, R. Maartens, P. Papodopoulos, and V. Rezanian, Phys. Lett. B **487**, 1 (2000).
 - [3] R. Maartens, Living Rev. Relativity **7**, 7 (2004).
 - [4] C. R. Keeton and A.O. Petters, Phys. Rev. D **73**, 104032 (2006).
 - [5] C. R. Keeton and A. O. Petters, Phys. Rev. D **72**, 104006 (2005). **73**, 044024 (2006).
 - [6] V. Bozza, Phys. Rev. D **66**, 103001 (2002).
 - [7] E. F. Eiroa, Phys. Rev. D **71**, 083010 (2005).
 - [8] R. Whisker, Phys. Rev. D **71**, 064004 (2005).
 - [9] S. Pal and S. Kar, Classical Quantum Gravity **25**, 045003 (2008).
 - [10] L. Iorio, Classical Quantum Gravity **22**, 5271 (2005).
 - [11] C.G. Böhmer, T. Harko, and F. S. N. Lobo, Classical Quantum Gravity **25**, 045015 (2008).
 - [12] A. Kotrlová, Z. Stuchlik, and G. Török, Classical Quantum Gravity **25**, 225016 (2008).
 - [13] C. S. J. Pun, Z. Kovács, and T. Harko, Phys. Rev. D **78**, 084015 (2008).
 - [14] E. Hackmann, V. Kagramanova, J. Kunz, and C. Lämmerzahl, Phys. Rev. D **78**, 124018 (2008).
 - [15] L.Á. Gergely, B. Darázs, arXiv:astro-ph/0602427v1 (2006).
 - [16] L.Á. Gergely, Z. Keresztes, M. Dwornik, arXiv:0903.1558v1 [gr-qc] (2009).
 - [17] A. N. Aliev and A. E. Gümrükçüoğlu, Phys. Rev. D **71**, 104027 (2005).
 - [18] R. da Rocha and C. H. Coimbra-Araujo, PoS, IC2006 **065** (2006).
 - [19] B. J. Ahmedov and F. J. Fattoyev, Phys. Rev. D **78**, 047501 (2008).
 - [20] R.M. Wald, Phys. Rev. D **10**, 1680 (1974).
 - [21] A. A. Abdujabbarov, B. J. Ahmedov, and V. G. Kagramanova, Gen. Rel. Grav. **40**, 2515 (2008).
 - [22] A.N. Aliev and V.P. Frolov, Phys. Rev. D **69**, 084022 (2004).
 - [23] N. Dadhich and Z.Ya. Turakulov, Classical Quantum Gravity **19**, 2765 (2002).
 - [24] A.F. Zakharov, Classical Quantum Gravity **11**, 1027 (1994).
 - [25] C. W. Misner, K.S. Thorne, and J.A. Wheeler, *Gravitation* (San Francisco: Freeman, 1973).
 - [26] R. Shafee, J. E. McClintock, R. Narayan, S. W. Davis, L.-X. Li, and R. A. Remillard, Astrophys. J. **636**, L113 (2006).
 - [27] R. Shafee, R. Narayan, and J. E. McClintock, Astrophys. J. **676**, 549 (2008).

(Dated: August 19, 2018)

Abstract

